

Computer Simulation of Ultrashort-Pulse Reflectometry in Helical Plasmas

FUKUCHI Atsushi, HOJO Hitoshi, ITAKURA Akiyoshi and MASE Atsushi¹

Plasma Research Center, University of Tsukuba, Tsukuba 305-8577, Japan

¹*Art, Science and Technology Center for Cooperative Research, Kyushu University, Kasuga 816-8580, Japan*

(Received: 9 December 2003 / Accepted: 2 June 2004)

Abstract

The two-dimensional full-wave simulations on ultrashort-pulse reflectometry for helical plasmas are studied based on the finite difference time domain (FDTD) method. The propagation of an ultrashort-pulse electromagnetic wave in helical plasmas is demonstrated, and the effect of strong magnetic shear in wave propagation is briefly discussed. The density-profile reconstruction is performed with use of the Abel inversion for the reflected waves from plasma, and it is shown that the reconstructed density profile coincides well with the original profile.

Keywords:

reflectometry, ultrashort pulse, helical plasma, FDTD method, computer simulation

1. Introduction

Millimeter-wave diagnostics such as reflectometry are receiving growing attention in magnetic confinement fusion research. In order to obtain the better understanding of plasma confinement physics, more detailed measurements on density profile and its fluctuations might be required. Recently, a new type of microwave reflectometry has been proposed, which is called as ultrashort-pulse reflectometry with use of subcyclic pulses being expected as a near-coming diagnostic [1-3]. A subcyclic pulse is a ultra-wide-band wave, and it can be considered as a set of monochromatic plane waves with various frequencies corresponding to various cutoff densities, therefore, the ultrashort-pulse reflectometry has a potential of measuring precisely the profiles of plasma density and magnetic field by only a single pulse. The theoretical studies on this ultrashort-pulse reflectometry have been also reported [4-7].

In this paper, we study two-dimensional full-wave simulation on ultrashort-pulse reflectometry for helical plasmas. The simulation scheme is based on the finite difference time domain (FDTD) method [8], and an analytic model obtained in ref. [9] is assumed for the helical magnetic field configuration. The outline of our simulation model is described in the following section, and in Sec. 3, the computational results on the wave propagation of an ultrashort pulse in LHD(Large Helical Device) plasma are shown. It seems that the obtained wave profiles manifest the strong shear effect of the helical magnetic field. The density profile reconstruction by ultrashort-pulse reflectometry with use of the Abel inversion is

also demonstrated in Sec. 4 and it is shown that the ultrashort-pulse reflectometry can work successfully for helical plasmas.

2. Simulation model

In this section, we describe the two-dimensional simulation modeling developed in refs. [7,8]. The basic equations to be solved are Maxwell's equations for the electromagnetic wave fields, \mathbf{E} and \mathbf{B} , and the equation of motion for the induced current density \mathbf{J} as follows:

$$\frac{\partial}{\partial t}\mathbf{B} = -\nabla \times \mathbf{E}, \quad (1)$$

$$\frac{\partial}{\partial t}\mathbf{E} = c^2\nabla \times \mathbf{B} - \frac{1}{\epsilon_0}\mathbf{J}, \quad (2)$$

$$\frac{\partial}{\partial t}\mathbf{J} = \epsilon_0\omega_{pe}^2\mathbf{E} - \frac{e}{m_e}\mathbf{J} \times \mathbf{B}_0, \quad (3)$$

where c is the speed of light, $\omega_{pe} (= (e^2n/m_e\epsilon_0)^{1/2})$ the electron plasma frequency, $-e$ the charge of the electron, m_e the electron mass, n the plasma density, ϵ_0 the permittivity of vacuum, and \mathbf{B}_0 is the external magnetic field being corresponding to the helical magnetic field. In the derivation of eq. (3), we assumed that the current density \mathbf{J} is approximated as $\mathbf{J} = -en_0\mathbf{v}_e$, \mathbf{v}_e being the electron flow velocity, as we consider electromagnetic waves in GHz range. The above coupled equations can describe both of the ordinary (O) and extraor-

dinary (X) modes in a plasma. When $\mathbf{B}_0 = B_0 \hat{z}$, \hat{z} being the unit vector in the z-direction, the wave component E_z denotes the O mode with the dispersion relation:

$$\omega^2 = \omega_{pe}^2 + c^2 k^2, \quad (4)$$

where k is the perpendicular wavenumber. On the other hand, E_x and E_y correspond to the X mode with the dispersion relation:

$$\left(\frac{kc}{\omega}\right)^2 = 1 - \frac{\omega_{pe}^2}{\omega^2} \frac{\omega^2 - \omega_{pe}^2}{\omega^2 - \omega_{pe}^2 - \omega_{ce}^2}, \quad (5)$$

where ω_{ce} is the electron cyclotron frequency. The cross polarization scattering between the O and X modes due to the magnetic shear is generated from the $\mathbf{J} \times \mathbf{B}$ term in eq. (3).

3. Wave propagation of ultrashort pulse

In this section, we show the computational results on the wave propagation of an ultrashort pulse in a helical plasma. We use an analytic expression shown in ref. [9] to describe the external magnetic field \mathbf{B}_0 for the LHD plasma, where the toroidal magnetic field is in the z-direction, and the poloidal magnetic field is in the x-y plane. We also assume the same parameters as ref. [9] for \mathbf{B}_0 . For the density profile, we assume

$$n(x, y) = \begin{cases} n_0 \left(1 - \frac{\psi(x, y)}{\psi_0}\right), & \psi \leq \psi_0, \\ 0, & \psi > \psi_0 \end{cases}, \quad (6)$$

where Ψ is a flux function, Ψ_0 denotes its value at the vacuum-plasma boundary, which is shown by an ellipse in each figure, and $n_0 = 5 \times 10^{12} \text{ cm}^{-3}$ is assumed for numerical calculations. We assume a Gaussian pulse with the full width at half maximum (FWHM) of 30 ps as the incident pulse, which is launched from the lower boundary in the y-direction ($y = -80 \text{ cm}$). We show the snapshots for the electric field profiles in Figs. 1-4. Figure 1 shows the electric wave field E_z of the

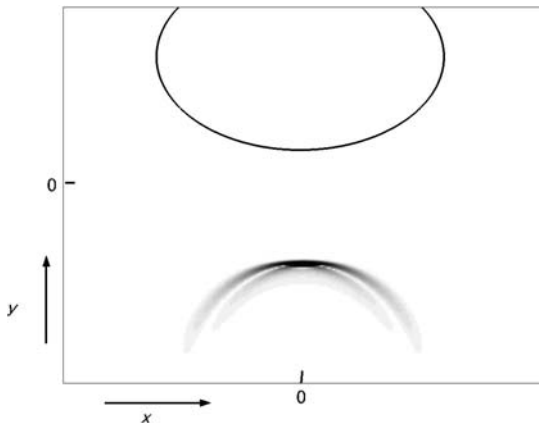


Fig. 1 The snap shot of an incident pulse (E_z).

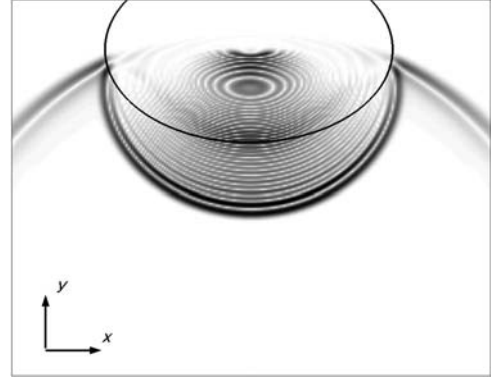


Fig. 2 The snap shot of the reflected wave (E_z).

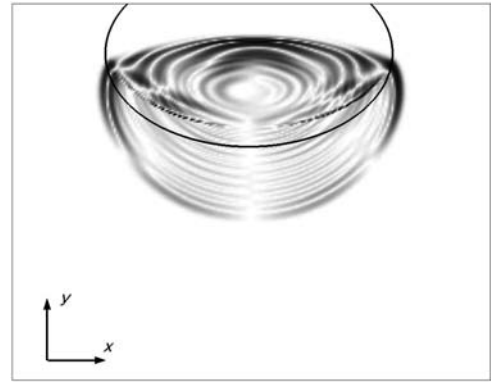


Fig. 3 The snap shot of E_y at the same time of Fig. 2.

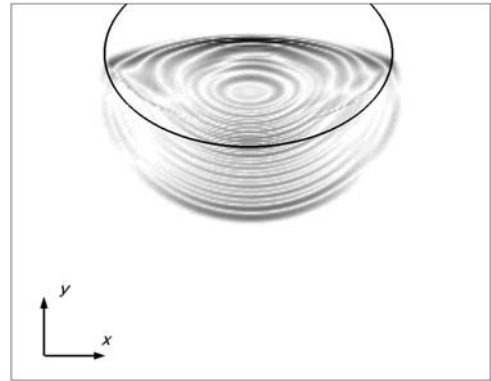


Fig. 4 The snap shot of E_x at the same time of Fig. 2.

incident pulse, and Figure 2 shows the reflected wave field E_z from the LHD plasma. We note that E_z is regarded to be approximately O-mode, as the toroidal field is much stronger than the poloidal field. Figures 3 and 4 correspond to the reflected wave fields E_y and E_x , respectively, at the same time as Fig. 2. For the reflected wave, we see that E_z is almost symmetric with respect to the central line of $x = 0$, on the other hand, E_y and E_x are not symmetric with respect to the line of $x = 0$. It is considered that the asymmetry in E_y and E_x

is due to the strong magnetic shear of the helical field.

4. Density profile reconstruction

We now analyze the density profile reconstruction by the measurement of the wave reflected at the cutoff. In Fig. 5, we show the temporal behavior of the electric wave field $E_z(t)$ observed at a position of $x = y = 0$. In the figure, the earlier large signal shows the incident pulse and the later signal denotes the reflected waves from the LHD plasma. From these reflected wave signals, we can obtain the time delay $\tau(\omega)$ as a function of ω as shown in Fig. 6, where open circles denotes the time delay $\tau(\omega)$ computed from the zero crossing method [4,7] and the solid line shows the curve fitted by a nonlinear optimization method [10]. By using the Abel inversion equation [4,7] defined by

$$x_r(\omega_{pe}) = \int_0^{\omega_{pe}} d\omega \frac{c\tau(\omega)}{\pi\sqrt{\omega_{pe}^2 - \omega^2}} \quad (7)$$

with $\tau(\omega)$ shown in Fig. 6, we can reconstruct the density profile $n(r)$. The reconstructed profile is shown in Fig. 7 by

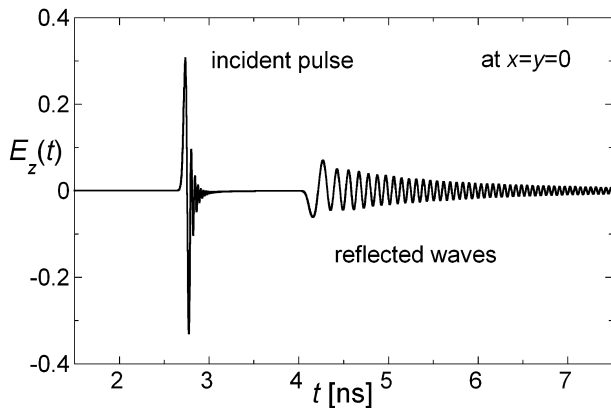


Fig. 5 The wave signal of E_z as a function of t detected at $x = y = 0$.

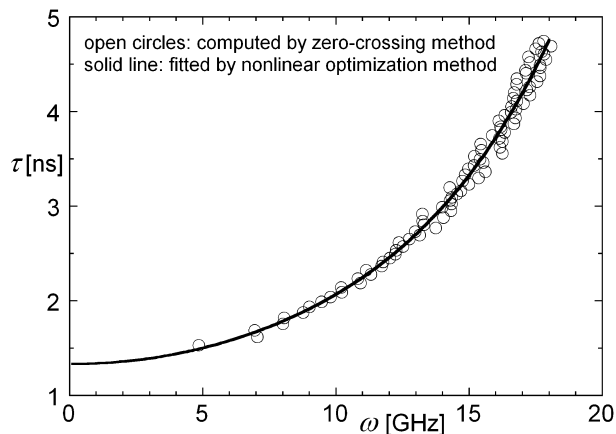


Fig. 6 The delay time τ of the reflected wave as a function of ω .

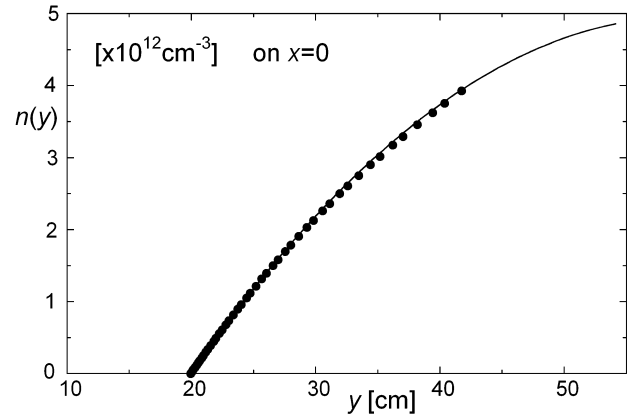


Fig. 7 The reconstructed density profile (closed circles). The solid line denotes the original density profile.

closed circles, where the solid line denotes the original density profile. We see that the reconstructed density profile coincides well with the original profile.

Finally, as the reflected wave E_z is spreading out widely, we can expect the possibility of imaging reflectometry for the multi-dimensional measurement of the density profile by using a detector array.

Acknowledgments

This work was partly performed as a collaborating program at National Institute for Fusion Science. The part of this work is also supported by Effective Promotion of Joint Research with Industry, Academia, and Government in Special Coordination Funds for Promoting Science and Technology, MEXT. The simulations were partly performed by the super computer of Science Information Processing Center, University of Tsukuba.

References

- [1] C.W. Domier *et al.*, Rev. Sci. Instrum. **66**, 399 (1995).
- [2] S. Kubota *et al.*, Jpn. J. Appl. Phys. **37**, L300 (1998).
- [3] S. Kubota *et al.*, Jpn. J. Appl. Phys. **38**, L202 (1999).
- [4] B.I. Cohen *et al.*, Plasma Phys. Control. Fusion **37**, 329 (1995).
- [5] B.I. Cohen *et al.*, Phys. Plasmas **6**, 1732 (1999).
- [6] H. Hojo *et al.*, Fusion Eng. Des. **34-35**, 447 (1997).
- [7] H. Hojo *et al.*, Rev. Sci. Instrum. **70**, 983 (1999).
- [8] H. Hojo *et al.*, J. Plasma Fusion Res. **78**, 387 (2002).
- [9] T. Watanabe and H. Akao, J. Plasma Fusion Res. **73**, 186 (1997).
- [10] L.C.W. Dixon, *Nonlinear Optimisation* (The English Universities Press, 1972).